

# Ab-initio Study of the Trimethylaluminum Atomic Layer Deposition Process on Carbon Nanotubes — An Alternative Initial Step

Anja Förster<sup>‡,†,•</sup>, Christian Wagner<sup>§</sup>, Jörg Schuster<sup>†,\*</sup> and Joachim Friedrich<sup>‡</sup>

<sup>‡</sup> *Technische Universität Chemnitz, 09126 Chemnitz, Germany*

<sup>†</sup> *Fraunhofer Institute for Electronic Nano Systems (ENAS), Chemnitz, Germany*

<sup>§</sup> *Center for Microtechnologies (ZfM), TU Chemnitz, Chemnitz, Germany and*

<sup>•</sup> *now at: TU Dresden, Center for Advancing Electronics Dresden (cfaed), 01062 Dresden*

Electronic applications of carbon nanotubes (CNTs) require the deposition of dielectric films on the tubes while conserving their excellent electronic properties. In our density functional theory study we use the trimethylaluminum (TMA) atomic layer deposition (ALD) as a model process for a CNT-functionalization. Since this functionalization relies on the presence of OH-groups, the CNTs are exposed to a water or oxygen pre-treatment. We show that only CNTs with a single-vacancy defect are able to react with H<sub>2</sub>O or O<sub>2</sub>. Further, the defect is preferably saturated by oxygen. This leaves the CNT without the necessary hydroxyl groups for the first TMA addition. Therefore, we propose an alternative initial step after which a classical TMA ALD process can be performed on the CNT.

## I. INTRODUCTION

Carbon nanotubes (CNTs) are characterized by an outstanding mechanical strength in combination with a high charge carrier mobility. The latter property makes them promising candidates for novel nano scale transistors, especially for high frequency applications [1, 2], interconnects [3, 4] or optoelectronic devices [5–8]. Their conductance is also very sensitive to external influences such as mechanical strain [9–12] or changes in their chemical environment promoting sensor applications as well [6, 8, 13–15]. The electronic properties of carbon nanotubes are closely related to their structure. Depending on their chiral angle, nanotubes can be metallic, semiconducting or semimetallic [16]. However, any application of CNTs relies on well defined electronic properties and thus type selected CNTs are required. Despite of ongoing research, there is lack of type selected material today. This is due low yield in complicated fabrication setups [17, 18] or expensive chirality sorting procedures after fabrication [19–21]. Thus, tuning the electronic properties of CNTs by deposition of functional thin films is seen as a promising approach. In addition, many device architectures based on carbon nanotubes rely on the possibility to deposit high quality dielectric films on CNTs, i.e. as gate isolation.

From a chemical perspective, carbon nanotubes are nearly perfect, rolled up graphene sheets. Graphene is known to be chemically inert, but CNTs show some reactivity which increases with curvature. This is due to a release of stress energy during the reaction increasing with CNT curvature. Although there is a finite reactivity, any chemical modification of CNTs is challenging. This applies for the deposition of functional films on CNTs by chemical vapor deposition as well.

Deposition of thin films by atomic layer deposition

(ALD) has been proven to yield uniform and conformal high quality films with a precise thickness control on many substrates as well as on nanostructures. In particular, ALD of Al<sub>2</sub>O<sub>3</sub> based on trimethylaluminum (TMA) and water is known to be a very robust process which is well studied in literature [22, 23]. Like many ALD methods the TMA ALD process relies on the existence of functional groups on the initial surface before the first ALD cycle can be performed. Specifically, hydroxyl groups must be present on the CNT which is the crux of the problem.

Different approaches for the TMA ALD on CNTs have been suggested in literature [24–28]. For example, Zhan et al. reported in their experimental study [27] that a pre-treatment with ethanol and sodium dodecylsulfate increases the ratio of hydroxylated surfacegroups. Consequently, this pre-treatment leads to a more conformal coating in comparison to the CNT being dispersed in water only. Farmer and Gordon [26] suggested an alternative way of performing a TMA ALD on CNTs which relies on nitrogen dioxide (NO<sub>2</sub>) being evenly adsorbed on the CNT's surface. In the following step TMA molecules react with the oxygen atoms of NO<sub>2</sub>, forming a uniform layer over the CNT. While effective, both methods introduces other atomic species such as sulfur and nitrogen.

Therefore, in our density functional theory (DFT) study we analyze an alternative pre-treatment of CNTs in a water and oxygen atmosphere that does not introduce any additional atomic species. Our pre-treatment requires the presence of single vacancy (SV) defects, which make the CNT more reactive [29]. This defect, characterized by a missing carbon atom, often occurs in chemical vapor deposition (CVD) grown CNTs [30]. According to [31] a defect rate up to 5% can be observed. We study the functionalization of metallic single wall (5,5)-CNTs via TMA ALD. Quantum chemical methods are used to obtain a thorough understanding of the CNT pre-treatments required prior to ALD-functionalization as well as the relevant process steps. In the second part of our study, the reaction pathways of the first steps of

\* joerg.schuster@enas.fraunhofer.de



TMA-ALD growth on the hydroxylized CNTs are analyzed and compared to similar reactions on flat substrates. We successfully show that TMA ALD performs well on pre-functionalized CNTs without introducing external atomic species such as nitrogen and sulfur.

## II. MODEL SYSTEM AND COMPUTATIONAL DETAILS

### A. Model System

Our model system is a metallic, non-periodic (5,5)-CNT consisting of five unit cells, leading to an overall CNT length of 12.3Å. The open ends are saturated with hydrogen atoms. Furthermore, the model system contains one SV defect and thus its chemical structure is  $C_{99}H_{20}$ . The presence of the SV defect turns the model CNT into an open-shell system. The calculation of the electronic structure of open shell systems requires multi reference methods. Such multi reference methods are computationally very expensive and are thus not suitable for large systems. Therefore, we avoid the open-shell-character by saturating the SV defect with oxygen, hydrogen or hydroxyl groups during the pre-treatment. Because of this saturation, the electronic structure of our model systems can be investigated by DFT, which is numerically cheaper than multi reference methods. From the technological perspective this approach is justified in any case as an unsaturated defect will instantly react with surrounding water or oxygen.

The avoidance of open shell systems in the electronic structure calculations has an important consequence for calculating the reaction energies of the pre-treatment reactions. Instead of comparing the energies of the pre-treated CNT with the bare defective CNT, we have to choose one of the pre-treated systems as the reference point for energy calculations. Due to the manifold of different reaction possibilities at the CNT defect, a systematic and intuitive labeling of the structures and the reactions is not trivial. We decided for a naming scheme based on the reaction type (cf. fig. 2): Structures A1-I1 are pre-treated structures ( $CNT + O_2$ ), where D1 is the one with the lowest energy and serves as a reference point for the energy calculations [32] (cf. fig. 1). A2-I2 are educts after wet oxygen reaction ( $CNT + O_2 + H_2O$ ), A3-I3 the educts after water reaction ( $CNT + 2H_2O$ ) and A4-I4 are structures after reaction with oxygen and two water molecules ( $CNT + O_2 + 2H_2O$ ).

According to this, reaction energies of the pre-functionalization are calculated as:

$$E_R = E_{pre-CNT} + E_{O_2} - E_{CNT-D1} - E_{func} \quad (1)$$

where  $E_{pre-CNT}$  is the energy of the pre-functionalized CNT and  $E_{CNT-D1}$  is the energy of the functionalized reference structure D1.  $E_{O_2}$  is the energy of oxygen which acts as our the reference functional group.  $E_{func}$

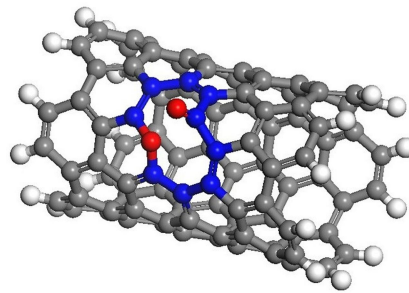


Figure 1. (Color online) Saturated CNT-structure D1 which functions as the reference point for all calculated reaction energies of the pre-treated CNTs. The atoms constructing the SV defect are highlighted in blue.

is the energy of the functional group of the actual functionalization reaction under consideration.

### B. Computational Details

In our DFT study Accelry's Materials Studio (Version 6.0) [33] and Turbomole (Version 6.3) [34] are used. Materials Studio is used for the calculation of the TMA ALD process, whereas Turbomole is used for high-throughput calculations of the CNT pre-treatment structures. In detail, the calculation setups are the following:

For the calculations with Turbomole the BP86 functional [35–39] together with the def2-SVP basis set for geometry optimization and frequency analysis is used. The Resolution of Identity (RI) approximation is applied to save calculation time [40]. On top, higher accuracy energy calculations with the def2-TZVP basis set [40, 41] are performed. The SCF energy convergence criterion is set to  $10^{-6}$  Ha while the geometry convergence is set to  $10^{-4}$  Ha for both basis sets.

Table I. Overview of the calculation details.

	TurboMole	Materials Studio
Functional	BP86	PBE
Basis set (geo. optimization)	Def2-SVP	DNP
Basis set (total energy)	Def2-TZVP	DNP
Scf criteria	$10^{-6}$ Ha	$10^{-5}$ Ha
Geometry opt. criteria	$10^{-4}$ Ha	$10^{-4}$ Ha
Orbital cutoff	—	4.8 Å
Smearing	—	$\leq 0.005$ Ha

Within Materials Studio Dmol<sup>3</sup> [42, 43] is used for the electronic structure calculations of the molecular systems. The functional of choice was PBE [44] which is used along with the DNP basis set [42], whose accuracy is similar to the def2-TZVP basis set of Turbomole [45]. The convergence criteria for the SCF energy calculations



is set to  $10^{-5}$  Ha and  $10^{-4}$  Ha for the geometry optimizations while the orbital cutoff is fixed at 4.8 Å. Due to convergence problems Fermi-Dirac-smearing with a maximum value of 0.005 Ha have been applied for some calculations. For a number of reference systems, the results of Dmol<sup>3</sup> and Turbomole have been compared in order to make sure that both codes give identical results within the expected error range (cf. App. A3 of [46]). The settings of both DFT codes are summarized in table I. For all reactions the whole CNT is allowed to relax.

### III. RESULTS AND DISCUSSION

#### A. CNT Pre-treatment

Deposition of thin films by ALD relies on the presence of functional groups on the surface. In the case of alumina ALD by using TMA as a precursor, hydroxyl groups are required. Consequently, we study the pre-treatment of defective CNTs in a reactive atmosphere consisting of oxygen and water prior to the actual TMA-ALD process.

In detail, we analyze reactions of one SV-defect on the (5,5)-CNT with 1) one oxygen molecule 2) one oxygen and one water molecule, 3) two water molecules and 4) with one oxygen and two water molecules (cf. fig. 2). The different reactions may result in the CNT possessing 1) two oxygen atoms, 2) one oxygen and two hydroxyl groups, 3) two hydroxyl groups and two hydrogen atoms or 4) four hydroxyl groups as functional groups. The reaction of the CNT with oxygen alone does not result in a hydroxylation. However, its energetics has to be considered in order to determine if a hydroxylation or an oxidation is preferable in case of concurrent reactions.

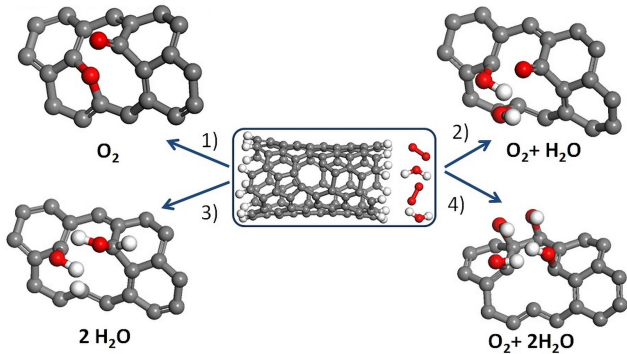


Figure 2. (Color online) a) Schematic illustrations of reactions 1)-4).

The SV-defect offers 9 positions where reactions can occur (see fig. 3a for illustration). In total, four bonds can be formed on the defect site. All positions are likely to form a single bond, except of position 1, where a double valence is preferred. Among the different positions,

number 1 has shown to be the most reactive during a pre-screening of the reactive sites. Thus, we focus on reaction configurations where position 1 is involved while the remaining sites are varied systematically around the defect. Table II gives an overview about the index of the structure and the according reaction sites. Figure 3b illustrates the different configurations exemplary for reaction 1) which involves two oxygen atoms. For the case of reaction 4) only a few typical configurations have been calculated in our study since the number of possible configurations is very high. Explicit structures of the correspondence of sites and functional groups are provided in the supporting material (see figure A.1, A.2 and A.3).

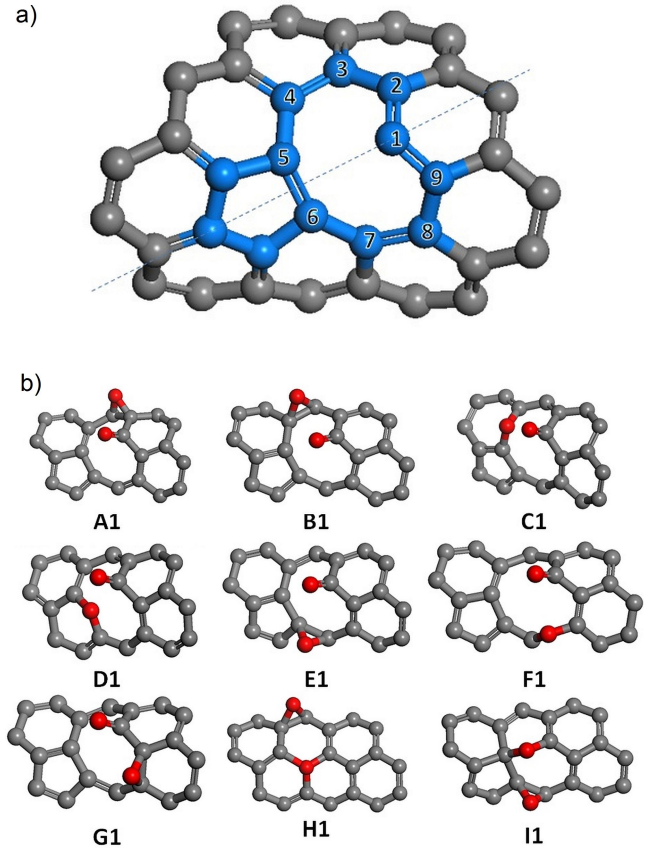


Figure 3. (Color online) a) Naming schemes of the carbon sites. The SV defect is highlighted in blue and the dashed line displays the mirror symmetry axis. b) Illustration of reaction 1) for the configurations A-I.

The calculated reaction energies for the different pre-treatment reactions (cf. eq. 1) are shown in fig. 4. The figure illustrates that the reaction energy depends on the type of the functional groups as well as on their position at the SV defect. Using configuration D1 (configuration D and reaction 1) as the reference, all other studied functionalization reactions yield higher positive values of the reaction energy. We can conclude that this reference reaction of the configuration D1 is proven to be the most stable structure throughout all studied reactions.



Table II. Naming scheme for the configurations and the involved carbon sites on the SV-defect, Double bonded sites are shown in bold. The carbon sites are displayed in fig. 2.

Configuration	Carbon sites	
	Reaction 1, 2, 3	Reaction 4
A	<b>1</b> , 2, 3	—
B	<b>1</b> , 3, 4	1, 2, 3, 4
C	<b>1</b> , 4, 5	1, 3, 4, 5
D	<b>1</b> , 5, 6	—
E	<b>1</b> , 6, 7	1, 5, 6, 7
F	<b>1</b> , 7, 8	—
G	<b>1</b> , 8, 9	1, 7, 8, 9
H	1, 3, 4, 5, 6	—
I	1, 5, 6, 7	—
K	—	1, 3, 5, 6
L	—	1, 5, 6, 8

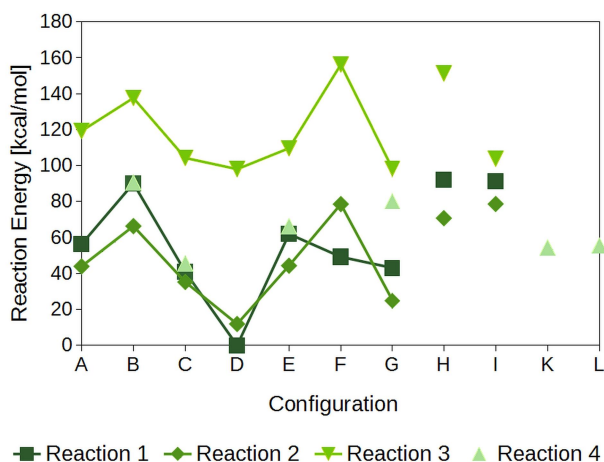


Figure 4. (Color online) Reaction energies of all studied pre-treatment reactions. Dark green for reaction 1 (oxygen molecule), medium green for reaction 2 (oxygen and water molecules), light green for reaction 3 (2 water molecules) and very light green for reaction 4 (oxygen and 2 water molecules). For reactions 1-3 the symbols for configuration A-G are connected due to the anti-clockwise movement of the functional groups (cf. fig. 3b and table II)

The dominating influence of the type of the functionalization reaction on the reaction energy is clearly visible in fig. 4. The energies of reaction 3), involving water only, are significantly higher than those of the reactions 1), 2) and 4) involving oxygen which all yield similar reaction energies for most of the positions. The difference of about 75 kcal/mol can be explained by comparing the sum of the binding energies of all bonds which are broken and formed in the course of these reactions. While the net bonding of reactions 1) and 2) and 4) are comparable and lie in the range of 220-230 kcal/mol, it reaches only 154 kcal/mol for reaction 3) which is indeed by 66-76 kcal/mol lower. We conclude that reactions involving oxygen are more likely to occur and that the formation of C-H groups is unfavorable in a mixed oxygen/water

atmosphere.

Besides the influence on the type of functionalization reaction, fig. 4 shows a clear dependence of the reaction energy on the configuration of the involved sites. Surprisingly, the position dependence of the reaction energy appears to be nearly identical for all four reactions. It is clearly visible in fig. 4 that the position dependence of the reaction energies reflects the mirror symmetry of the single vacancy defect (cf. fig. 3a). The most symmetric configuration D is the lowest in energy for the reactions 1), 2) and 3). It is characterized by double bonds at the carbon position 1 and two single bonds situated at the opposite carbon positions. Around the defect structure, the configurations A/G, B/F and C/E should be identical which is true for our data within the typical accuracy range of the DFT results.

Besides the systematic variation of the carbon positions around the defect structure, a few other configurations have been studied which are also shown in fig. 4. These configuration were chosen in accordance to the low energy of D1, where the oxygen atom not only supplies the missing electrons, but also re-completes one hexagon ring of the defect (see in fig. 3b). Based on the configurations H and I, we can conclude that the double bond at the carbon atom 1 is of crucial importance for the reaction energy (cf. fig. 3a). Reaction 1) and 2) allow for such a double bond to be formed at atom 1. However, due to steric hindrance it is impossible for two hydroxyl groups to bind to carbon atom 1 in reaction 4). Surprisingly this does not significantly raise the overall reaction energy of reaction 4).

In contrast, replacing the double bonded oxygen atom at position 1 with one hydrogen atom and one hydroxyl group in case of reaction 3) increases the reaction energy. This is the effect of the repulsion between the hydrogen atom and hydroxyl group at the carbon atom 1. Configuration I illustrates this clearly. Opposed to A-F, in I1, I2 and I3 no double bonded oxygen atom is present at carbon atom 1, bringing the energies for reaction I1, I2 and I3 closer together than for any other configuration.

In conclusion, our pre-treatment study shows that the carbon atom, where the functional group is bound to, influences the reaction energy. This conclusion results in the fact that structure D1 is the most stable one, as the carbon atom 1 is double bonded to an oxygen atom.

The next step is to either investigate whether it is possible to perform the TMA-ALD without the presence of hydroxyl groups similar to some exceptional cases on metal surfaces [47, 48] or to find a way to hydroxylate the CNT. The first possibility is briefly explained in the next section.

In the latter case this can be achieved either by finding an energetic more favorable structures saturated by hydroxyl groups or by finding a reaction path that turns this oxygen defect into a hydroxylated one. Since the first approach is not straight forward and includes the investigation of a wide variety of structures, we decided to follow the latter option.



## B. TMA ALD Process Performed on CNTs

In order to obtain the required hydroxyl groups for the initial TMA ALD step, we let the dominant pre-treated CNT configuration D1 react with water. In our simulations the water molecules are forced to react with the functional groups and not with the CNT itself. Under these conditions, we are able to bond water molecules via hydrogen bonds to the oxygen atom of the D1 structure (see fig. 5). This structure is further referred to as  $D1_{H_2O}$ .

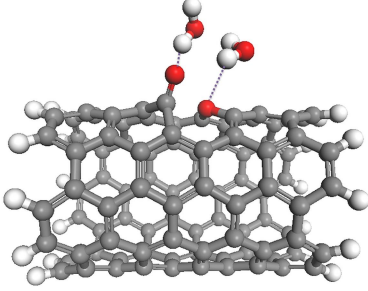


Figure 5. (Color online) Two water molecules bound to the dominant oxygen structure D1, forming  $D1_{H_2O}$ .

The investigated reactions show that the bonding of the water molecules to the oxygen atom is energetically favorable by 5 kcal/mol per bonded water molecule. In the resulting structure the water molecules are close enough to the SV defect of the CNT such that they can function as hydrogen donors for the reaction with TMA.

For the course of the ALD reactions the chemisorption of TMA has to be checked. As a concurrent reaction the water may react with TMA prior to its adsorption on the oxygen-functionalized defect D1. Thus we investigate whether the TMA molecule, as desired, is able to bond to  $D1_{H_2O}$ .

In fig. 6 we show the detailed reaction pathway for the first and second TMA molecule reacting with  $D1_{H_2O}$ . The zero point reference energy for this reaction part is the educt  $D1_{H_2O}$  (cf. fig. 5). All reaction energies are calculated with reference to this system. Thus, the reaction energy  $E_R$  is defined as:

$$E_R = E_{nCNT} + m * E_{CH_4} - E_{(n-1)CNT} - E_{TMA}, \quad (2)$$

with  $E_{nCNT}$  being the energy of the CNT after the  $n$ -th ALD sub-step,  $E_{(n-1)CNT}$  the energy of the CNT before the  $n$ -th ALD sub-step,  $m$  is the number of the created methyl groups and  $E_{TMA}$  the energy of the TMA-precursor.

Fig. 6 shows that in the first reaction step the TMA molecule reacts with the oxygen atom that shares a double bond with carbon atom 1. The replacement of the C=O bond with a C-O-Al bond to create  $TS_1$  (transition state 1) is exothermic by 33.3 kcal/mol. In a next

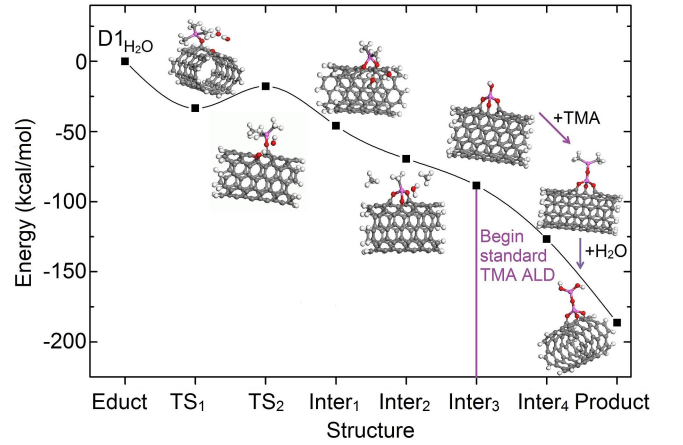


Figure 6. (Color online) The alternative reaction pathway for the TMA ALD process. Beginning with the educt  $D1_{H_2O}$  two TMA molecules react one after another with the CNT, forming transition states (TS) and intermediate states (Inter) until the final product is formed. The purple line indicates where the standard TMA ALD process starts. first with the TMA addition, followed by the reaction of water.

step, one of the two water molecules donates one hydrogen atom to form the first  $CH_4$  molecule. The remaining hydroxyl group of the water molecule bonds with carbon atom 6, forming  $TS_2$ . The reaction barrier for this step (cf. fig. 6) is 15.6 kcal/mol. This barrier height is in good agreement with the literature value of about 12 kcal/mol [22].

We also investigated the reaction of TMA with the non-hydroxylated CNT D1, which is presented in detail in the appendix. We found that while the reaction energy for the first transition state  $TS_1$  is similar between  $D1_{H_2O}$  and D1, the further reaction steps for the non-hydroxylated CNT D1 are less favorable.

During the following two reaction steps the aluminum atom is further anchored to the middle of the SV defect. From  $TS_2$  to  $Inter_1$  (intermediate state 1) the oxygen atom of the initial D1 turns towards the aluminum atom and the newly introduced hydroxyl group reacts with methyl to release a second  $CH_4$  molecule (cf.  $Inter_2$  in fig. 6).

The reaction of the second water molecule with the precursor results into the structure  $Inter_3$ , which completes the reaction of the first TMA molecule with the CNT at -88.5 kcal/mol. The resulting structure obtains one hydroxyl group, which is the seed for a standard TMA ALD cycle. The new cycle does not rely on the presence of nearby water molecules anymore. According to [23] the addition of one TMA molecule is an exothermic reaction by 39 kcal/mol. This is in agreement with our value of the reaction energy for the addition of the second TMA molecule (38.3 kcal/mol). A similar agreement is found for the second ALD half cycle where two water molecules from the gas phase react with  $Inter_4$  to the final product of our investigation. For this step literature [23] predicts



an energy of 68 kcal/mol, which is in the same range as our DFT reaction energy of 58.8 kcal/mol.

We can conclude that it is possible to bond one aluminum atom to the oxidized CNT defect by ALD via adsorbed water molecules, which form hydrogen bonds to the oxygen atoms. Once this first TMA molecule is bound to the CNT, a seed is provided from where a standard TMA ALD process can be performed.

#### IV. CONCLUSIONS

We present a study on the reaction of a metallic, non-periodic (5,5)-CNT with a SV defect in a wet oxygen atmosphere. We show that the reaction energy of a number of pre-functionalization reactions symmetrically depends on the position of the functional groups, wherein carbon atom 1 takes a special position in the symmetry axis (cf. fig. 3a). While a saturation of the SV defect with 4 hydroxyl groups would be ideal, we demonstrate that a defective CNT preferably reacts with oxygen.

In order to functionalize such an oxidized CNT via TMA ALD, water molecules have to be adsorbed via hydrogen bonds to the oxygen atoms of the defect. These water molecules act as the hydrogen donors for the first TMA ALD step. Once this step is successfully completed, a standard TMA ALD cycle can be performed on the CNT with hydroxyl groups on the first deposited aluminum atom acting as the seed.

As the basis for this alternative TMA ALD process relies on the SV defect of the CNT, we can generalize this process for other metallic and semiconducting CNTs containing SV defects. This method could also be used as an initial step for other ALD processes that rely on hydroxyl groups, but where only oxygen is present on the surface.



- 
- [1] M. Steiner, M. Engel, Y.-M. Lin, Y. Wu, K. Jenkins, D. B. Farmer, J. J. Humes, N. L. Yoder, J.-W. T. Seo, A. A. Green, M. C. Hersam, R. Krupke, P. Avouris, *Appl. Phys. Lett.* **101**, 053123 (2012).
- [2] M. Schröter, M. Claus, P. Sakalas, M. Haferlach, D. Wang, *IEEE J. Electron Devices Soc.* **1**, 9 (2013).
- [3] H. Fiedler, M. Toader, S. Hermann, R. D. Rodriguez, E. Sheremet, M. Rennau, S. Schulze, T. Wächtler, M. Hietschold, D. R. Zahn, et al., *Micro. Eng.* **120**, 210 (2014).
- [4] H. Fiedler, M. Toader, S. Hermann, M. Rennau, R. D. Rodriguez, E. Sheremet, M. Hietschold, D. R. Zahn, S. E. Schulz, T. Gessner, *Micro. Eng.* **137**, 130 (2015).
- [5] N. Rauhut, M. Engel, M. Steiner, R. Krupke, P. Avouris, A. Hartschuh, *ACS Nano* **6**, 6416 (2012).
- [6] M. Scarselli, P. Castrucci, M. D. Crescenzi, *J. Phys.: Condens. Matter* **24**, 313202 (2012).
- [7] P. Avouris, M. Freitag, V. Perebeinos, *Nat. Photon* **2**, 341 (2008).
- [8] T. Blaudeck, D. Adner, S. Hermann, H. Lang, T. Gessner, S. E. Schulz, *Micro. Eng.* **137**, 135 (2015).
- [9] L. Yang, J. Han, *Phys. Rev. Lett.* **85**, 154 (2000).
- [10] A. Kleiner, S. Eggert, *Phys. Rev. B* **63**, 073408 (2001).
- [11] C. Wagner, J. Schuster, T. Gessner, *Phys. Stat. Sol. B* **249**, 2450 (2012).
- [12] C. Wagner, J. Schuster, T. Gessner, *J Comput Electron* **15**, 881 (2016).
- [13] J. Lefebvre, J. Fraser, Y. Homma, P. Finnie, *Appl. Phys. A* **78**, 1107 (2004).
- [14] Y. Ohno, S. Iwasaki, Y. Murakami, S. Kishimoto, S. Maruyama, T. Mizutani, *Phys. Rev. B* **73**, 235427 (2006).
- [15] V. Sgobba, D. M. Guldi, *Chem. Soc. Rev.* **38**, 165 (2009).
- [16] M. P. Anantram, F. Léonard, *Rep. Prog. Phys.* **69**, 507 (2006).
- [17] R. Rao, D. Liptak, T. Cherukuri, B. I. Yakobson, B. Maruyama, *Nat. Mater.* **11**, 213 (2012).
- [18] F. Yang, X. Wang, D. Zhang, J. Yang, LuoDa, Z. Xu, J. Wei, J.-Q. Wang, Z. Xu, F. Peng, X. Li, R. Li, Y. Li, M. Li, X. Bai, F. Ding, Y. Li, *Nature* **510**, 522 (2014).
- [19] A. A. Green, M. C. Hersam, *Adv. Mat.* **23**, 2185 (2011).
- [20] H. Liu, T. Tanaka, Y. Urabe, H. Kataura, *Nano Lett.* **13**, 1996 (2013).
- [21] T. Tanaka, Y. Urabe, T. Hirakawa, H. Kataura, *Anal. Chem.* **87**, 9467 (2015).
- [22] S. M. George, *Chem. Rev.* **110**, 111 (2010).
- [23] M. Knez, N. Pinna, *Atomic Layer Deposition of Nanostructured Materials*, (WILEY-VCH Verlag, Weinheim, 2011).
- [24] J. Lee, B. Min, K. Cho, S. Kim, J. Park, Y. Lee, N. Kim, M. Lee, S. Park, J. Moon, *J. Cryst. Growth* **254**, 443 (2003).
- [25] C. Herrmann, F. Fabreguette, D. Finch, R. Geiss, S. George, *Appl. Phys. Lett.* **87**, 123110 (2005).
- [26] D. B. Farmer, R. G. Gordon, *Nano Lett* **6**, 699 (2006).
- [27] G.-D. Zhan, X. Du, D. M. King, L. F. Hakim, X. Liang, J. A. McCormick, A. W. Weimer, *J Am Ceram Soc* **91**, 831 (2008).
- [28] A. S. Cavanagh, C. A. Wilson, A. W. Weimer, S. M. George, *Nanotechnology* **20**, 255602 (2009).
- [29] M. Kozłowska, J. Goclón, P. Rodziewicz, *Appl Surf Sci* **362**, 1201310 (2016).
- [30] R. Rao, A. E. Islam, N. Pierce, P. Nikolaev, B. Maruyama, *Carbon* **95**, 287 (2015).
- [31] D. B. Mawhinney, V. Naumenko, A. Kuznetsova, J. T. Yates, J. Liu, R. Smalley, *Chem. Phys. Lett.* **324**, 213 (2000).
- [32] The formation energy of this structure from the CNT with the SV defect is about -165 kcal/mol and therefore highly exothermic.
- [33] Accelrys Software Inc., *Materials Studio Release Notes, Release 6.0* (San Diego: Accelrys Software Inc., 2011).
- [34] TURBOMOLE V6.3 2011, a development of University of Karlsruhe and Forschungszentrum Karlsruhe GmbH, 1989-2007, TURBOMOLE GmbH, since 2007; available from <http://www.turbomole.com>.
- [35] J. P. Perdew, *Phys. Rev. B* **33**, 8822 (1986).
- [36] J. C. Slater, *Phys. Rev.* **81**, 385 (1951).
- [37] P. A. M. Dirac, *P R Soc London Ser-A* **123**, 714 (1929).
- [38] S. H. Vosko, L. Wilk, M. Nusair, *Can. J. Phys.* **58**, 1200 (1980).
- [39] A. D. Becke, *Phys. Rev. A* **38**, 3098 (1988).
- [40] F. Weigend, *Phys. Chem. Chem. Phys.* **8**, 1057 (2006).
- [41] F. Weigend, M. Häser, H. Patzelt, R. Ahlrichs, *Chem. Phys. Lett.* **294**, 143 (1998).
- [42] B. Delly, *J Chem Phys* **92**, 508 (1990).
- [43] B. Delly, *J Chem Phys* **113**, 7756 (2000).
- [44] J. P. Perdew, K. Burke, M. Ernzerhof, *Phys. Rev. Lett.* **77**, 3865 (1996).
- [45] B. Delly, *J Phys Chem A* **110**, 13632 (2006).
- [46] A. Förster, "Ab-initio studies of reactions to functionalize carbon nanotubes"(Bachelor thesis, TU Chemnitz, 2012).  
<http://nbn-resolving.de/urn:nbn:de:bsz:ch1-qucosa-103907>
- [47] J. Lu, B. Liu, N. P. Guisinger, P. C. Stair, J. P. Greeley, J. W. Elam, *Chem Mat* **26**, 6752 (2014).
- [48] S. S. Masango, R. A. Hackler, A.-I. Henry, M. O. McAnally, G. C. Schatz, P. C. Stair, R. P. Van Duyne, *J Phys Chem C* **120**, 3822 (2016).



## Appendix A: Supporting information

### 1. Position of functional groups

The following figures A.1 to A.3 show the position of the functional groups on the SV defect for the reactions 2)-4).

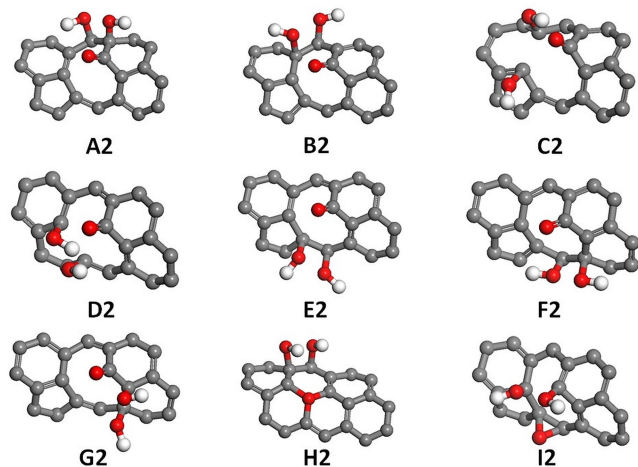


Figure A.1. (Color online) Positions of the functional groups for Reaction 2) with oxygen and one water molecule.

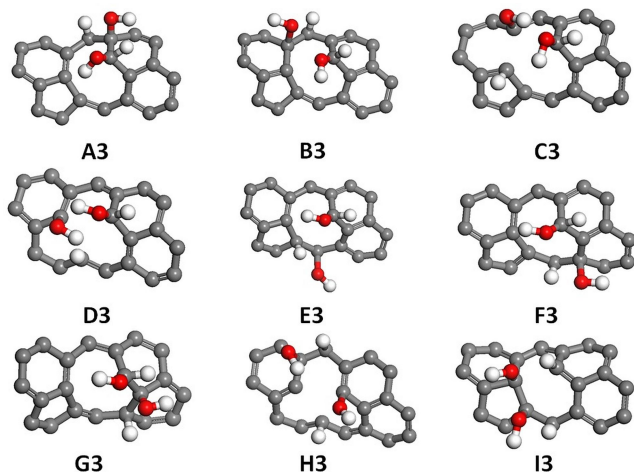


Figure A.2. (Color online) Positions of the functional groups for Reaction 3) with 2 water molecules.

### 2. TMA ALD on non-hydroxylated CNTs

Here, we want to briefly discuss the TMA ALD process that is performed on the dominant pre-treated CNT configuration D1 without the presence of water molecules. Figure A.4 shows a comparison of the first initial step between the configuration D1 and the hydroxylated struc-

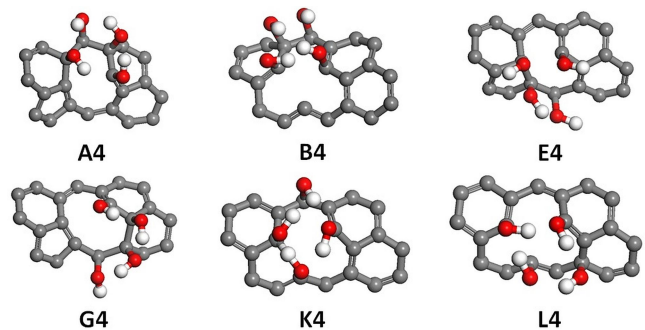


Figure A.3. (Color online) Positions of the functional groups for Reaction 4) with oxygen and 2 water molecules.

ture  $D1_{H_2O}$  as discussed in the sub-section IIIB. It is visible that while the transition states of D1 and  $D1_{H_2O}$  are similar in energy (-33.1 kcal/mol and -33.3 kcal/mol, respectively) the energy of the next reaction step differs.

The intermediate state  $Inter_1$  from the starting structure  $D1_{H_2O}$  is more stable (-44.8 kcal/mol) than the transition state  $TS_2$  of D1 (-30.6 kcal/mol). This makes the reaction with the starting structure  $D1_{H_2O}$  favorable. We note that 'analogous to the pre-treatment' the methyl group has many possible bonding sites, with the carbon atoms 1-9 of the SV defect being the most likely candidates. The structure as shown on figure A.4 is the reaction site which so far is the most promising. Further studies would be necessary to affirm this preliminary finding.

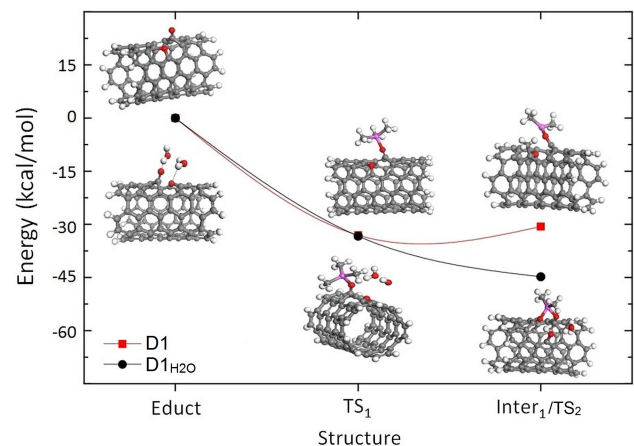


Figure A.4. (Color online) Comparison of the first TMA ALD reaction step on the structure D1 (red) and  $D1_{H_2O}$  (black). The pictures in the top half show the structure for the reaction with D1 and the structures in the bottom half belong to the reaction with  $D1_{H_2O}$ .

The methyl group that binds to the CNT at D1 takes away one possible anchor site for the TMA molecule, which makes the non-hydroxylated pathway less favorable. This can prevent the TMA molecule from forming a more stable bond/connection to the CNT. In the case



of  $D1_{H_2O}$ , on the other hand, it is possible to anchor up to two TMA molecules at the SV defect of the CNT (cf. fig. A.5).

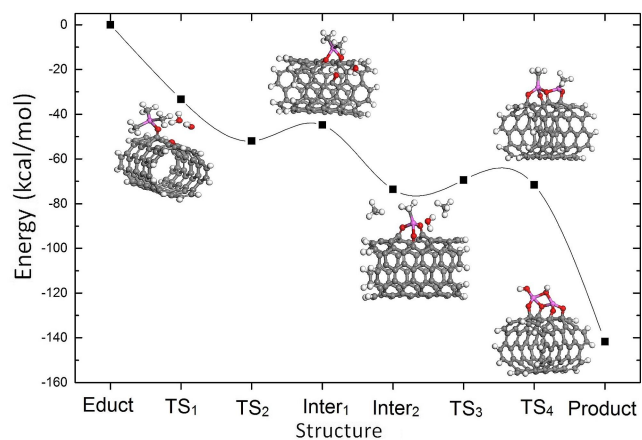


Figure A.5. (Color online) An alternative TMA ALD reaction of the educt  $D1_{H_2O}$  where 2 TMA molecules bind directly to the SV defect.